Journal of Inorganic Biochemistry 157 (2016) 25–33

Contents lists available at ScienceDirect

Journal of Inorganic Biochemistry

journal homepage: www.elsevier.com/locate/jinorgbio

Complexation and molecular modeling studies of europium(III)–gallic acid–amino acid complexes

Mohamed Taha, Imran Khan, João A.P. Coutinho *

CICECO—Aveiro Institute of Materials, Department of Chemistry, University of Aveiro, 3810-193 Aveiro, Portugal

ARTICLE INFO

Article history:
Received 27 July 2015
Received in revised form 6 January 2016
Accepted 18 January 2016
Available online 21 January 2016

Keywords:
Eu(III) complexes
Gallic acid
Amino acids
Stability constants
COSMO-RS
DFT

ABSTRACT

With many metal-based drugs extensively used today in the treatment of cancer, attention has focused on the development of new coordination compounds with antitumor activity with europium(III) complexes recently introduced as novel anticancer drugs. The aim of this work is to design new Eu(III) complexes with gallic acid, an antioxida'nt phenolic compound. Gallic acid was chosen because it shows anticancer activity without harming health cells. As antioxidant, it helps to protect human cells against oxidative damage that implicated in DNA damage, cancer, and accelerated cell aging. In this work, the formation of binary and ternary complexes of Eu(III) with gallic acid, primary ligand, and amino acids alanine, leucine, isoleucine, and tryptophan was studied by glass electrode potentiometry in aqueous solution containing 0.1 M $NaNO_3$ at (298.2 ± 0.1) K. Their overall stability constants were evaluated and the concentration distributions of the complex species in solution were calculated. The protonation constants of gallic acid and amino acids were also determined at our experimental conditions and compared with those predicted by using conductor-like screening model for realistic solvation (COSMO-RS) model. The geometries of Eu(III)–gallic acid complexes were characterized by the density functional theory (DFT). The spectroscopic UV–visible and photoluminescence measurements are carried out to confirm the formation of Eu(III)–gallic acid complexes in aqueous solutions.

1. Introduction

The DNA-binding metal complexes are an important fundamental issue in understanding metal-based drug in cancer chemotherapy, and can greatly help to design new and active anticancer drugs [1–3]. This binding interaction creates different types of cancer cell's DNA lesions, which blocks the division of cancer cells. Cisplatin (*cis*-$[PtCl_2(NH_3)_2]$) is among the most effective cancer chemotherapeutic drugs in treating various cancers, such as ovarian, head, neck and lung cancers, as well as several others [4,5]. Since the discovery of cisplatin as anticancer drug, there are thousands of platinum complexes that have been developed but few are available for clinical use [4,5]. Despite the success of platinum-based antitumor drugs, they have some major drawbacks that include severe toxicity, cisplatin-resistant tumors, and low solubility in aqueous solution [5]. More recently, lanthanide (Ln) coordination complexes have been attracting attention in bioinorganic chemistry and clinical research [6]. These complexes are of interest due to their therapeutic radioisotopes and luminescence properties. They are widely used in radioimmunotherapy and photodynamic therapy [7–10]. They have found therapeutic applications, such as osteoporosis, hyperphosphatemia, antiparasitic, and cancer treatment [11–15]. Ln complexes may provide a broader spectrum of antitumor activity as compared with classical platinum anticancer drugs. Europium(III) complexes with several ligands have been synthesized and investigated as new anticancer agents [16–19]. The high coordination number of Eu(III) ion (8 or 9) provides more coordination sites for DNA-binding, prompting strong interaction with DNA as compared with classical platinum anticancer drugs [20].

In this work, the complexation equilibrium between Eu(III) ion and the antioxidant gallic acid in aqueous solution was studied. Gallic acid can be found naturally in a wide-range of vegetables and fruits, such as tea, gallnuts, sumac, apple peels, strawberries, bananas, lemons, and pineapples [21]. It exists either in the free form or in the form of esters [22]. Besides being an efficient antioxidant, it has also many potential therapeutic applications, such as antibacterial [23], antiviral [24], kidney-protective [25], and cardio-protective [26] effects. Recently, gallic acid has been shown to have *in vitro* anticancer activity against various cancer cell lines, such as breast cancer [27], lung cancer [28,29], prostate cancer [30], bladder cancer [31], cervical cancer [32,33], esophageal cancer, gastric cancer and colon cancer [34], leukemia [35], osteosarcoma [36,37] and melanoma [38,39]. Moreover, gallic acid possesses a more selective cytotoxicity towards cancer cells than towards normal cells [35,40,41].

Gallic acid has shown to form highly stable complexes with di- and tri-valent metal ions in aqueous solution [42–44]. It is considered as simple model of catechol-type siderophore, which contains hydroxyl groups adjacent to the benzene ring. It has been proposed that

* Corresponding author.
E-mail address: jcoutinho@ua.pt (J.A.P. Coutinho).

http://dx.doi.org/10.1016/j.jinorgbio.2016.01.017
0162-0134/

siderophores have higher affinity for the trivalent metal ions than the divalent metal ions because of the higher charge density of the former ions [45]. Thus, gallic acid may form a strong complex with Eu(III) ion in water, helping to solve a major problem in a variety of different lanthanide(III) complexes, namely, the low stability in aqueous media. In some cases the Ln(III) complexes are prone to dissociation in water into "free ligand" form and hydrated lanthanide ions [46]. Aiming for developing stable Eu(III) complexes, the equilibria of Eu(III)–gallic acid complexes in aqueous solution and their stability constants were investigated by potentiometry. The complex formation between Eu(III)–gallic acid and some important amino acids [alanine (Ala), leucine (Leu), isoleucine (Ile), and tryptophan (Trp)] was also studied, and their overall stability constants in water determined. The protonation constants of gallic acid and amino acids were predicted theoretically using COSMO-RS model.

2. Experimental

2.1. Materials

Europium(III) nitrate pentahydrate (purity >99.9 wt.%) was supplied by Sigma-Aldrich. Gallic acid (purity >99.5 wt.%) was purchased from Merck. L-Alanine (purity >99.0 wt.%) was obtained from BDH. L-Leucine (purity >99.0 wt.%) and L-isoleucine (purity >99.0 wt.%) were supplied by Merck. L-Tryptophan (purity ≥99.5%) was obtained from Sigma-Aldrich. Sodium hydroxide pellets was obtained from Eka Chemicals. Nitric acid (65 wt.%), and potassium hydrogen phthalate (purity >99.8) were obtained from Panreac (Barcelona, Spain). Sodium nitrate (purity >99.5) was purchased from HiMedia Labs. Purified water was taken from a reverse osmosis and a Milli-Q plus 185 water purifying system and used in all experiments. The pure water was then degassed under vacuum at 70 °C and cooled under nitrogen gas atmosphere.

2.2. Potentiometric apparatus

The pH-potentiometric titration method was followed the IUPAC guidelines for apparatus [47] and measurement [48], as well as the critical evaluation of the reported stability constants [47,49]. The pH-titration measurements were carried out using an automatic titrator (Metrohm 904) equipped with an 801 magnetic stirrer, a Metrohm dosimat (model 683), Pt 1000/B/2 (Metrohm 6.1114.010), a pH glass electrode (Metrohm 6.0262.100) with a precision of ±0.001, and a personal computer. The titration vessel, a 70 ml double-walled glass cell, was connected to a thermostatic water bath to maintain the solution temperature at (298.2 ± 0.1) K. This vessel was sealed with a special lid containing various inlets for insertion of the electrode, burette tip, temperature probe, a nitrogen gas inlet and outlet. The titration vessel was provided with a magnetic stirrer bar. The Tiamo 2.3 software was employed to record and control the titration process.

2.3. Calibration of the potentiometric apparatus

The glass pH electrode was calibrated in terms of hydrogen ion concentration, p[H]. The method usually employed by a strong acid–strong base titration with no Eu(III) ion or ligand, but with background electrolyte solution. The calibration solution was prepared by adding 2 ml of 0.1 M HNO_3 and 50 ml of 0.1 M $NaNO_3$ solution in to the titration vessel. After temperature control at (298.2 ± 0.1) K has been reached and nitrogen gas has been established to remove CO_2 and O_2, and the stirrer has been started, the calibration solution is titrated with 0.1 M CO_2-free NaOH. The concentration of NaOH has a precisely standardized against potassium hydrogen-phthalate.

The electrode potential (E, mV) readings and NaOH increments (ml) were recorded with Tiamo 2.3 program. The calibration curve (*e.g.* Fig. S1a in the Supporting Information) is simply a plot of the observed electrode potential (mV) as a function of the NaOH volume (ml). This data was treated with GLEE software [50] to compute the standard electrode potential and slope of the Nernst equation [50] (Eq. (1)),

$$E = E^{\circ} + s\log\left[H^{+}\right]. \quad (1)$$

The selection of observed data to be used for the calibration is very important. The useable data was restricted to the pH ranges around 2.5–4.0 and 10.7–11.3. The E° and s were found to be 404.8 ± 0.6 and 59.04 ± 0.04 mV, respectively.

The presence of some carbonate in the calibration solution was estimated using Gran plot (*e.g.* Fig. S1b in the Supporting Information), and was found to be less than 1.0%. The ion-product constant of water (pK_w) under our experimental conditions (298.2 ± 0.1) K and ionic strength I = 0.1 M $NaNO_3$ is 13.78 [51], which was submitted as input to GLEE program.

2.4. The experimental runs

The total volume of the titration solution was 50 ml, and the NaOH solution was added in small increments of 0.025 ml to provide more than 150 experimental data points for each run. Each titration run was repeated three times, and simultaneously used for fitting. All measurements were carried out at (298.2 ± 0.1) K and ionic strength I = 0.1 M $NaNO_3$. The nitrogen gas was bubbled through the titration solution for 10 min before starting the titration, and the vessel was kept under a small positive pressure of N_2 to remove the dissolved CO_2 and O_2.

The first experimental run was made to determine the protonation constants of gallic acid and amino acids. The ligand concentration was 1×10^{-3} M and the acid concentration was 3×10^{-3} M HNO_3. The second run was conducted to calculate the stability constants of the binary complexes of Eu(III) with gallic acid or amino acids. The ligand concentration was 1×10^{-3} M and 1.2×10^{-3} M, and the Eu(III) concentration varied from 1×10^{-3} M to 4×10^{-4} M according to the Eu(III) to ligand ratios 1:1, 1:2.5 and 1:3. For our final experimental run, the Eu(III) ion with both ligands (gallic acid and amino acid) at molar ratio (1:1:1) was made to determine the stability constants of the ternary complexes. The concentration of Eu(III), gallic acid, or amino acid was 1×10^{-3} M.

2.5. Computation of protonation and stability constants

The determination of the protonation and stability constants was computed using the nonlinear least-squares computer program Hyperquad (Version 2008) [52]. After calculating the E° and slope s of the Nernst equation, the electrode potential (E, mV) readings were converted to p[H] readings and used together with NaOH increments (ml) as input data for the Hyperquad program. The algorithm involved in the Hyperquad program calculates p[H] directly by solving a set of nonlinear equations of mass-balance. The basic algorithm in Hyperquad can be stated as in Eq. (2),

$$T_i = [X_i] + \sum_{k=1,nk} q_{ik}\beta_k \prod_{j=l,nr} [X_j]^{qjk} \quad (2)$$

which is a statement of the mass balance at a given titration point of the i-th reagent ($i = 1, nr$). The $[X_i]$ and β are the free concentration of the i-th reagent and equilibrium constants, respectively. The objective function (U) of the refinement process to find equilibrium constants, which give the best fit to the experimental p[H], is given by Eq. (3),

$$U = \sum_{i=1,np} W_i r_i^2 \quad (3)$$

where W is the matrix of weights and r is a residual, which equal to the difference between experimental and calculated data of the p[H]. The model that exhibits the best statistical fit and, of course, more chemically sensible was chosen from a number of other possible models

of formed complexes. The species distribution diagrams (SDDs) of the formed complexes in the solution were calculated with the Hyperquad Simulation and Speciation (HySS 2009) program [53]. The SDD is a powerful visualization tool for the accurate assessment of all species present in solution and their concentrations as a function of p[H].

2.6. Photoluminescence spectra

The photoluminescence spectra were recorded at 300 K with a modular double grating excitation spectrofluorimeter with a TRIAX 320 emission monochromator (Fluorolog-3, Horiba Scientific) coupled to a R928 Hamamatsu photomultiplier, respectively, using a front face acquisition mode. The excitation source was a 450 W Xe arc lamp. The emission spectra were corrected for detection and optical spectral response of the spectrofluorimeter and the excitation spectra were corrected for the spectral distribution of the lamp intensity using a photodiode reference detector.

2.7. Spectrophotometric spectra

Absorption spectra were carried out by a UV–Vis spectroscopy Pharma-Spec Spectrometer, at 298.2 K.

2.8. Computational details

The theoretical calculations here reported comprise the study of the geometries of gallic acid, neutral (H_4GA), mono-, di-, tri-, and tetra-anions ($[H_3GA]^-$, $[H_2GA]^{2-}$, $[HGA]^{3-}$, and $[GA]^{4-}$) in the gas phase and in the conductor reference state (COSMO) by means of RI-DFT BP/COSMO method using the triple zeta valence plus polarization (TZVP) basis set with the TURBOMOLE 6.1 program [54]. The optimized geometries of the neutral, anionic, and zwitterionic forms of the amino acids were also performed at the same level of theory. The optimized geometries in the shape of energy and COSMO files were handed to COSMOtherm software version C30_1401 [55,56] in order to predict the dissociation constants of gallic acid and amino acids using from the linear free energy relationship (LFER) [57]. The σ-profiles of gallic acid and amino acid species are given in Figs. S2–S6 in the Supporting Information. The geometries of the Eu(III)–gallic acid complexes were fully optimized at the same level of theory, RI-DFT BP/COSMO-TZVP. The relativistic effective core potential (ECP) was used for Eu atom [58].

3. Results and discussion

3.1. Dissociation constants

The pH-potentiometric curves of Eu(III)-gallic acid-alanine system is depicted in Fig. 1, as an example and the other system are shown in Figs. S7–S9 in the Supporting Information. Gallic acid has four potential acidic protons, one carboxylic group and three phenolic (OH) groups capable of deprotonation [59]. The overall protonation constants, β_n, of H_4GA can be expressed as,

$$\beta_n = K_{a1}\cdot K_{a2}\cdots K_n = \frac{\left[H_nGA^{n-4}\right]}{\left[H^+\right]^n\left[GA^{-4}\right]} \quad (4)$$

where $n = 1$–4 and $K_{a1}\cdot K_{a2}\cdots K_n$ are the stepwise dissociation constants,

$$K_n = \frac{\left[H^+\right]\left[H_{n-1}GA^{1-n}\right]}{\left[H_nGA^{n-4}\right]}. \quad (5)$$

The carboxylic acid of the gallic acid is dissociated at 4.33 [42,44] and their three phenolic (OH) groups are deprotonated at 8.71 [42,44], 11.4 [60,61], and 12.8 [61]. The *pKa* values of gallic acid have been studied by different research groups, but only very few of them were able to calculated pK_{a3} and pK_{a4} values [60,61] due to their high basicity. It is difficult to determine accurately the pK_{a4} of gallic acid by p[H] measurements because raising the p[H] above 12 depasses the limit for the accurate p[H] range measurements, 2–12. Thus, our attention was focused on determining the $pK_{a1\text{-}3}$ values. An example of a gallic acid p[H] titration curve is shown in Fig. 1. Best fits were obtained when constants $pK_{a1\text{-}3}$were refined simultaneously. The overall protonation constants ($\log\beta_{1\text{-}3}$) and stepwise dissociation constants ($pK_{a1\text{-}3}$) of gallic acid were calculated with the Hyperquad program and reported in Table 1. The $pK_{a1\text{-}3}$ values are in good agreement with the previously published data [42,44,60,61]. The first dissociation constant ($pK_{a1} = 4.33$) involves the carboxylic group. It was found that the Gibbs free energy of the deprotonation from that central O–H bond is lower than the other two (O–H) bonds by 3.23 kcal·mol^{-1} [62]. Therefore, the second dissociation constant ($pK_{a2} = 8.98$) corresponds to the central hydroxyl group. The two dissociation constants (the pK_{a1} of the carboxyl group and the pK_{a2} of the amino group) of the amino acids were also determined and reported in Table 1 along with the literature data, which are all in excellent agreement with the literature values [63].

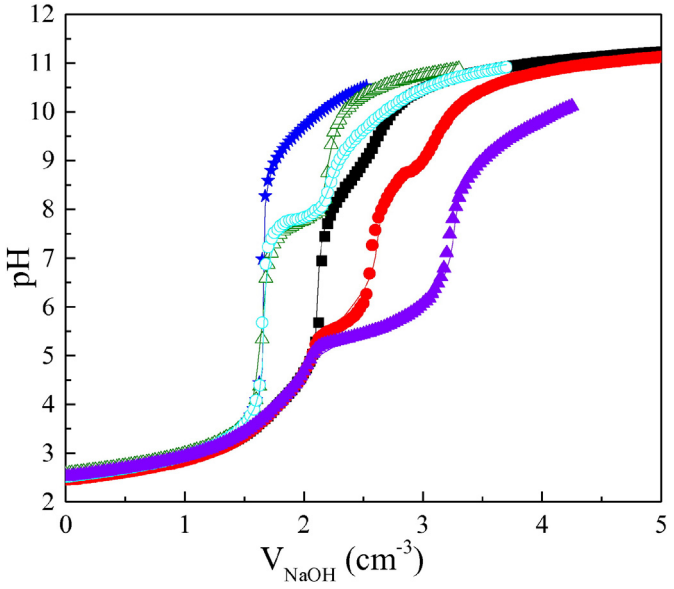

Fig. 1. Potentiometric titration curves of Eu–gallic acid–Ala system at $T = 298.2$ K and $I = 0.1$ M. The symbol and solid lines are the experimental and calculated data; (■) 1×10^{-3} M gallic acid, (★)1×10^{-3} M Ala, (Δ) 4×10^{-4} M Eu(III), (●) 4×10^{-4} M Eu(III) + 1×10^{-3} M gallic acid, (○) 4×10^{-4} M Eu(III) + 1×10^{-3} M Ala, and (▲) 1×10^{-3} M Eu(III) + 1×10^{-3} M gallic acid + 1×10^{-3} M Ala.

The prediction of *pKa* values of acids or bases using the implicit solvent model COSMO-RS does not require explicit solvent molecules [64,65]. The pK_{a2} values of gallic acid and the investigated amino acids in water were predicted using the pK_a-LFER method, as implemented in the COSMOtherm program,

$$pK_a^i = c_0 + c_1\left(\Delta G^i_{neutral} - \Delta G^i_{ion}\right) \quad (6)$$

where $c_0 = -113.01849$ and $c_1 = 0.10229$ mol·kJ^{-1}, the LFER constants. The $\Delta G^i_{neutral}$ and ΔG^i_{ion} refer to the Gibbs free energies of the neutral and the ionic species at infinite dilution in water, respectively. In the case of gallic acid, the pK_{a1}, pKa_2, pKa_3, and pKa_4 were calculated from the free energy difference of $G(H_4GA) - G(H_3GA^-)$, $G(H_3GA^-) - G(H_2GA^{2-})$, $G(H_2GA^{2-}) - G(HGA^{3-})$, $G(HGA^{3-}) - G(GA^{4-})$, respectively. The predicted $pK_{a1\text{-}4}^{COSMO}$ values of gallic acid using conductor-like screening model for realistic solvation (COSMO-RS) implicit solvation method are respectively 4.94, 8.57, 10.72, and 14.1. The results indicate that the first three ($pK_{a1\text{-}3}^{COSMO}$) values are in good agreement with the

Table 1
Protonation constants of gallic acid and amino acids in water at 298.2 K and ionic strength $I = 0.1$ M $NaNO_3$.

Amino acids	Logβ_1	Logβ_2	Logβ_3	pK_{a1}^{exp}	pK_{a1}^{COSMO}	pK_{a2}^{exp}	pK_{a2}^{COSMO}	pK_{a3}^{exp}	pK_{a3}^{COSMO}
Gallic acid	11.12 ± 0.08	20.10 ± 0.08	24.43 ± 0.08	4.33 ± 0.08	4.94	8.98 ± 0.08	8.57	11.12 ± 0.08	10.72
Alanine	9.69 ± 0.01 (9.72)[a]	11.91 ± 0.07 (12.05)[a]	–	2.22 ± 0.07	2.63	9.69 ± 0.01	9.26	–	–
Leucine	9.60 ± 0.04 (9.66)[a]	12.07 ± 0.13 (11.98)[a]	–	2.47 ± 0.13	2.84	9.60 ± 0.04	8.80	–	–
Isoleucine	9.56 ± 0.01 (9.65)[a]	11.80 ± 0.18 (11.93)[a]	–	2.24 ± 0.18	2.47	9.56 ± 0.01	9.04	–	–
Tryptophan	9.23 ± 0.05 (9.34)[a]	11.73 ± 0.10 (11.74)[a]	–	2.50 ± 0.10	1.60	9.23 ± 0.05	8.90	–	–

[a] Ref. [63].

experimental values with an error of less than ±0.6 pK_a units, while the pK_{a4}^{COSMO} is 1.2 pK_a units higher than the experimental value. The fully optimized structures of the neutral and anionic conformers involved in the dissociation equilibrium of gallic acid are shown in Fig. 2. As reported in Table 1, the COSMO-RS model was also shown to be accurate for predicting the pK_{a1}^{COSMO} and pK_{a2}^{COSMO} values of the studied amino acids, with values less than ±0.5 pK_a unit; expect the pK_{a1}^{COSMO} value of tryptophan was lower than the pK_{a1}^{exp} with 1.1 pK_a unit

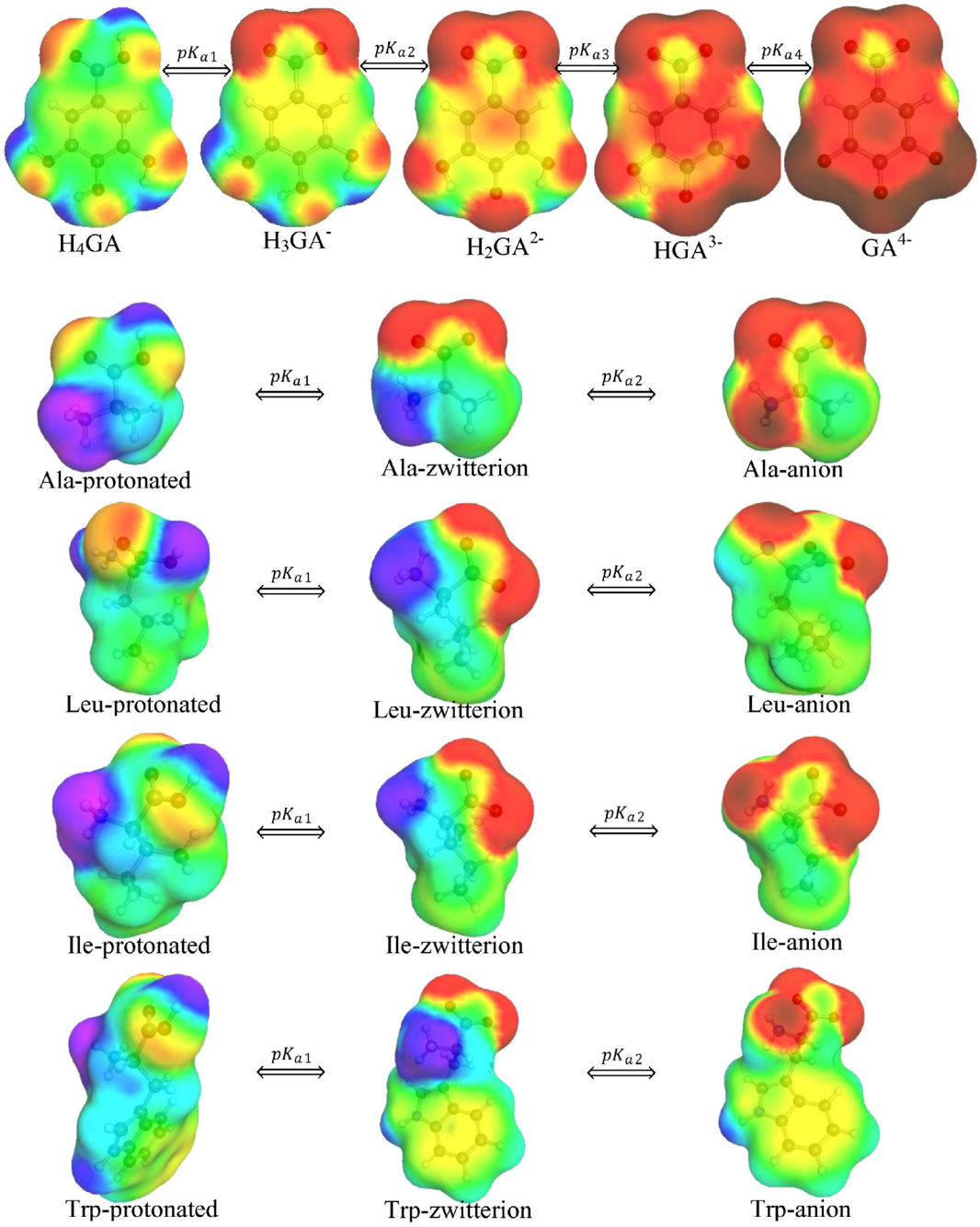

Fig. 2. Depiction of sigma surface and geometries of gallic acid and amino acid ions. The color codes of the negative and positive polar regions are deep red and deep blue, respectively.

and the pK_{a2}^{COSMO} value leucine was lower that the experimental value with 0.8 pK_a unit. The optimized structures of amino acid ions are also shown in Fig. 2.

3.2. Eu(III) complex formation

The overall stability constants, β_{pqr}, for the species $(Eu(III)_p(Gallic\ acid)_q(amino\ acid)_rH_s)$ formed in the solution between Eu(III), gallic acid, amino acid, and proton (H) are defined in Eq. (7); the charges are omitted for clarity.

$$p\mathrm{Eu(III)} + q(\text{Gallic acid}) + r(\text{Amino acid}) + sH \rightleftharpoons \mathrm{Eu(III)}_p(\text{Gallic acid})_q(\text{Amino acid})_rH_s,$$

$$\beta_{pqrs} = \frac{\left[\mathrm{Eu(III)}_p(\text{Gallic acid})_q(\text{Amino acid})_rH_s\right]}{[\mathrm{Eu(III)}]^p[\text{Gallic acid}]^q[\text{Amino acid}]^r[H]^s} \quad (7)$$

where p, q, r, and s are the stoichiometric coefficients of the solution species Eu(III), gallic acid, amino acid, and H^+ ions, respectively, and the square-bracket symbol refers to molar concentration. The p, q, r, and s values are positive integers or zero, a positive value for s refers to the protonated complexes. Additionally, s can have a negative value corresponding to the deprotonated or the hydroxo-complexes. The overall stability constants, $\log\beta_{pqrs}$, of the speciation models that best described the pH titration data of the binary and ternary complexes are given in Table 2.

The mononuclear hydroxo-complexes, $Eu(OH)_n^{3-n}$ ($n = 0$–4), in water have been previously studied [66] at $I = 0$ and $T = 298.15$ K. The potentiometric titration of 0.0004 M $Eu(NO_3)_3$ in aqueous solution at 298.2 K and $I = 0.1$ M $NaNO_3$ is shown in Fig. 1. This titration data was fitted to the reaction model previously established in aqueous solution, which involved mononuclear hydroxo-complexes (Table 1). The equilibrium constants of $Eu(OH)^{2+}$, $Eu(OH)_2^+$, $Eu(OH)_3$, and $Eu(OH)_4^-$ are in good agreement with previously reported values [66]. The distribution of Eu(III) hydroxo complexes in 0.1 M $NaNO_3$ using their stability constants is illustrated in Fig. 3. The Eu(III) ion exists in hydrate form until ~ pH 5. The hydrolysis of the Eu(III) ion increases above this pH. In the pH range from 5 to 10, the $Eu(OH)^{2+}$ and $Eu(OH)_2^+$ species coexist but do not exceed 40% and 27%, respectively. The $Eu(OH)_3$ is the dominant species at ~pH 10.2. The $Eu(OH)_4^-$ becomes a predominant species at pH > 12.5.

The refinement of the potentiometric data of gallic acid with Eu(III) ion indicates the formation of $[Eu(H_2GA)]^+$, $[Eu(HGA)]$, $[Eu(HGA)_2]^{3-}$, and $[Eu(HGA)_3]^{6-}$ complexes, and their overall stability constants (Table 2) clearly indicate that gallic acid forms strong complexes with Eu(III) ion. The protonation constants of gallic acid and the hydrolysis constraints of Eu(III) ion were introduced to the Hyperquad program as constants in the refinement. The stepwise stability constants (logK) were calculated to show how tightly gallic acid is bound to Eu(III). The $\log K_{Eu(HGA)}$, $\log K_{Eu(HGA)_2}$, and $\log K_{Eu(HGA)_3}$ values are 11.33, 5.90, and 4.29, respectively, which $\log K_{Eu(HGA)} = \log\beta_{1100}$, $\log K_{Eu(HGA)_2} = \log\beta_{1200} - \log\beta_{1100}$, and $\log K_{Eu(HGA)_3} = \log\beta_{1300} - \log\beta_{1200}$. The values of the stepwise stability constants follow the order of $\log K_{Eu(HGA)_3} < \log K_{Eu(HGA)_2} < \log K_{Eu(HGA)}$, indicating that the first gallic acid molecule binds more tightly to the Eu(III) ion than the second and the third ones, and this is expected from the statistical and steric considerations. This was further supported by the optimization of these complexes using the RI-DFT-BP/COSMO method using TZVP basis set and a relativistic ECP on the Eu atom. Gallic acid was treated as a bidentate ligand since metal–gallic acid chelation mostly occurs between two adjacent hydroxyl groups. In aqueous solution, an equilibrium exists between $[Eu(H_2O)_8]^{3+}$ and $[Eu(H_2O)_9]^{3+}$. The 8-fold coordinated Eu(III) species in water was used in the optimization. The metal–ligand binding energies (ΔE_{bind}) for the $Eu(HGA)(H_2O)_6$, $Eu(HGA)_2(H_2O)_4^{3-}$, and $Eu(HGA)_3(H_2O)_2^{6-}$ complexes are (−43.62, −23.56, and −21.65) kcal·mol^{-1}, respectively, where $\Delta E_{bind} =$

Table 2
The overall stability constants ($\log\beta_{pqrs}$) for Eu(III) complexes with gallic acid and amino acids at 298.15 K and ionic strength $I = 0.1$ M $NaNO_3$.

Complex species	$Eu_p(gallic\ acid)_q(AA)_rH_s$				$\log\beta_{pqrs}$	SD
	p	q	r	s		
Eu(III)						
$[Eu(OH)]^{+2}$	1	0	0	−1	−7.76 (−7.64)[a]	0.14
$[Eu(OH)_2]^+$	1	0	0	−2	−15.98 (−15.1)[a]	0.08
$[Eu(OH)_3]$	1	0	0	−3	−24.05 (−23.7)[a]	0.08
$[Eu(OH)_4]^-$	1	0	0	−4	−36.37 (−36.2)[a]	0.34
Gallic acid complexes						
$[Eu(H_2GA)]^+$	1	1	0	1	17.29	0.07
$[Eu(HGA)]$	1	1	0	0	11.33	0.04
$[Eu(HGA)_2]^{3-}$	1	2	0	0	17.23	0.06
$[Eu(HGA)_3]^{6-}$	1	3	0	0	21.52	0.11
Gallic acid and alanine complexes						
$[Eu(Ala)]^{2+}$	1	0	1	0	4.72 (4.7)[a]	0.07
$[Eu(HGA)(Ala)H]$	1	1	1	1	25.23	0.01
$[Eu(HGA)(Ala)]^-$	1	1	1	0	16.00	0.01
$[Eu(HGA)(Ala)H_{-1}]^{2-}$	1	1	1	−1	5.90	0.02
Gallic acid and leucine complexes						
$[Eu(Leu)]^{2+}$	1	0	1	0	4.56 (4.27)[b]	0.06
$[Eu(HGA)(Leu)H]$	1	1	1	1	24.68	0.04
$[Eu(HGA)(Leu)]^-$	1	1	1	0	15.85	0.03
$[Eu(HGA)(Leu)H_{-1}]^{2-}$	1	1	1	−1	5.51	0.06
Gallic acid and isoleucine complexes						
$[Eu(Ile)]^{2+}$	1	0	1	0	4.45	0.06
$[Eu(HGA)(Ile)H]$	1	1	1	1	24.94	0.03
$[Eu(HGA)(Ile)]^-$	1	1	1	0	15.70	0.04
$[Eu(HGA)(Ile)H_{-1}]^{2-}$	1	1	1	−1	5.67	0.06
Gallic acid and tryptophan complexes						
$[Eu(Trp)]^{2+}$	1	0	1	0	4.42 (4.29)[b]	0.06
$[Eu(HGA)(Trp)H]$	1	1	1	1	24.68	0.02
$[Eu(HGA)(Trp)]^-$	1	1	1	0	15.66	0.03
$[Eu(HGA)(Trp)H_{-1}]^{2-}$	1	1	1	−1	5.73	0.04

[a] Ref. [66]; ($I = 0$; $T = 298.15$ K).
[b] Ref. [63].

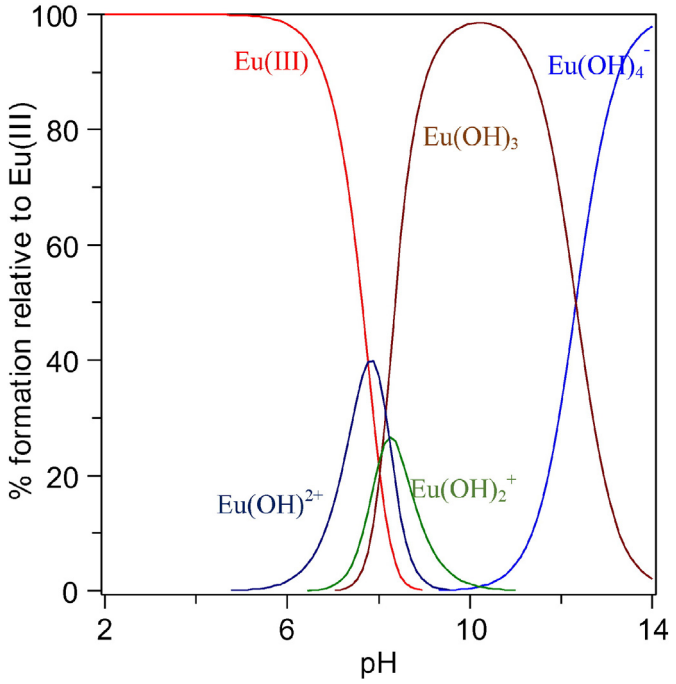

Fig. 3. Species-distribution diagram of $4 \cdot 10^{-4}$ M Eu(III) in 0.1 M $NaNO_3$ as a function of pH at 298.2 K.

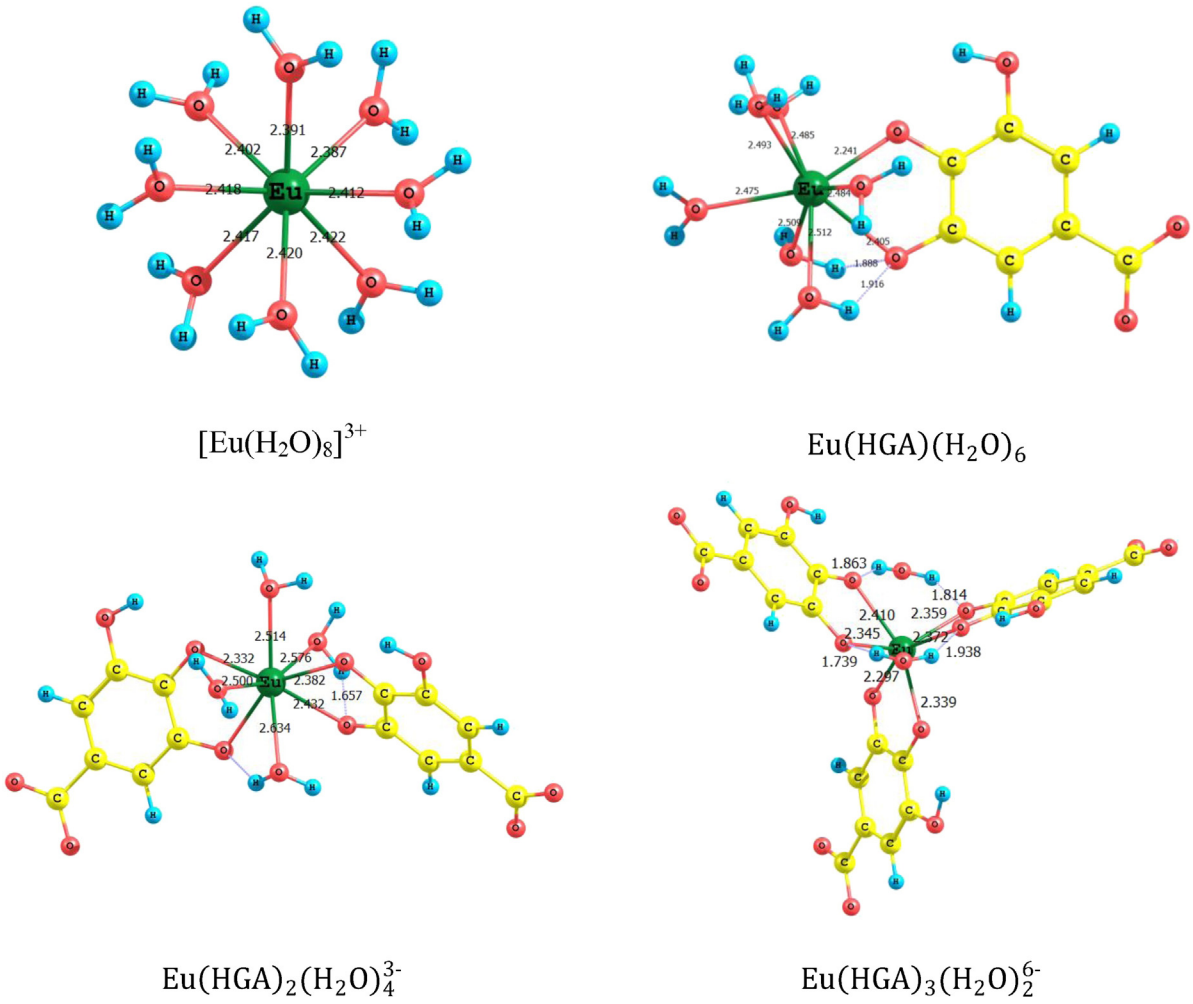

Fig. 4. The optimized structures of $[Eu(H_2O)_8]^{3+}$, $Eu(HGA)(H_2O)_6$, $Eu(HGA)_2(H_2O)_4^{3-}$, and $Eu(HGA)_3(H_2O)_2^{6-}$ complexes with DFT/TZVP levels. The atom distances are in angstroms.

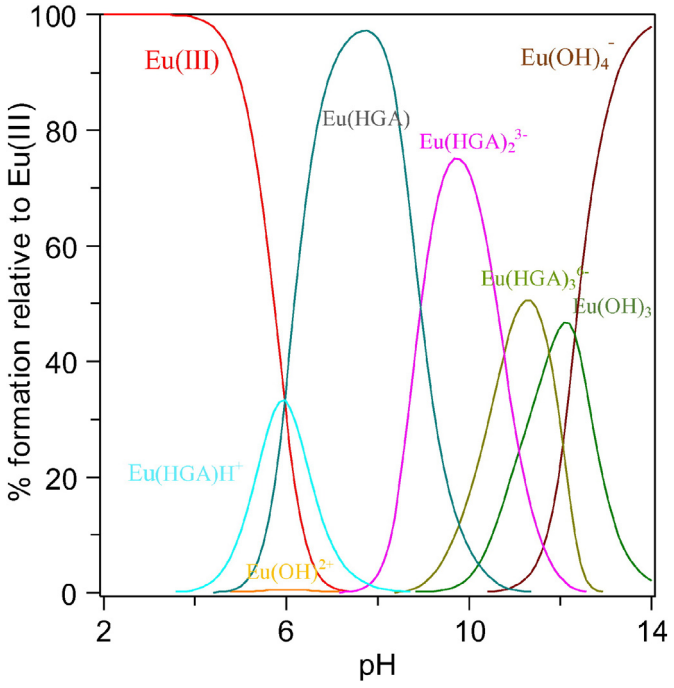

Fig. 5. Species-distribution diagram of $4 \cdot 10^{-4}$ M Eu(III) + $1 \cdot 10^{-3}$ M gallic acid in 0.1 M $NaNO_3$ as a function of pH at 298.2 K.

$\sum E_{products} - \sum E_{reactants}$ for Eqs. (8)–(10). The obtained ΔE_{bind} values follow the same order of the stepwise stability constants. The optimized structure of the $Eu(HGA)(H_2O)_6$, $Eu(HGA)_2(H_2O)_4^{3-}$, and

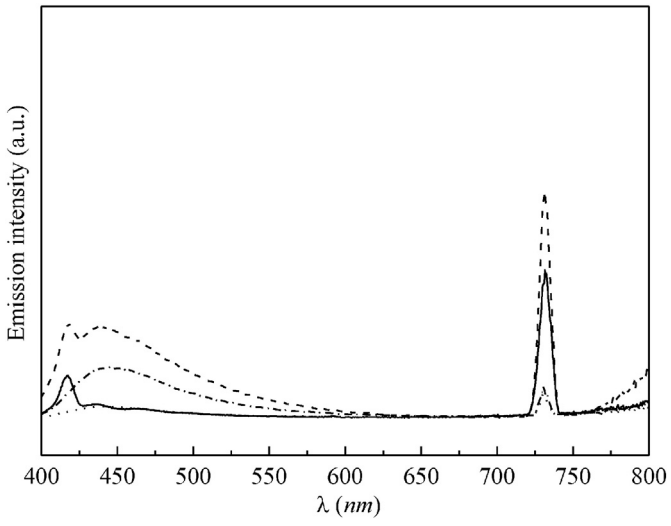

Fig. 6. Emission spectra of (solid line; 1×10^{-3} M $EuCl_3 \cdot 6H_2O$), (dash line; 1×10^{-3} M $EuCl_3 \cdot 6H_2O$ + 1×10^{-3} M gallic acid, at pH 8.0), (dot line; 1×10^{-3} M $EuCl_3 \cdot 6H_2O$ + 2×10^{-3} M gallic acid, at pH 9.8), and (dash dot line; 1×10^{-3} M $EuCl_3 \cdot 6H_2O$ + 3×10^{-3} M gallic acid, at pH 11.4), under excitation at 365 nm at 298.2 K.

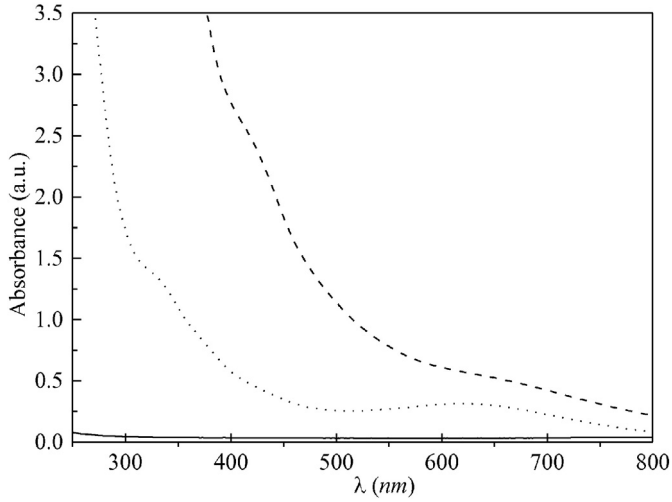

Fig. 7. Absorption spectra for (solid line; 1×10^{-3} M $EuCl_3 \cdot 6H_2O$), (dot line; 1×10^{-3} M gallic acid, at pH 9.8), and (dash line; 1×10^{-3} M $EuCl_3 \cdot 6H_2O + 2 \times 10^{-3}$ M gallic acid, at pH 9.8) at 298.2 K.

$Eu(HGA)_3(H_2O)_2^{6-}$ complexes are shown in Fig. 4, and their sigma surface is given in Fig. S10 in the Supporting Information.

$$Eu(H_2O)_8^{3+} + HGA^{3-} \Leftrightarrow Eu(HGA)(H_2O)_6 + 2H_2O, \quad (8)$$

$$Eu(HGA)(H_2O)_6 + HGA^{3-} \Leftrightarrow Eu(HGA)_2(H_2O)_4^{3-} + 2H_2O, \quad (9)$$

$$Eu(HGA)_2(H_2O)_4^{3-} + HGA^{3-} \Leftrightarrow Eu(HGA)_3(H_2O)_2^{6-} + 2H_2O, \quad (10)$$

The species distribution diagram (SDD) computed for the conditions of Fig. 5 at 1:2.5 molar ratio reveals that gallic acid is a very strong chelator for Eu(III), which the [Eu(HGA)] species predominates, interesting, at the physiological pH ~ 7.4, with concentration reached *ca.* 97% to the total Eu(III). Above this pH, the $[Eu(HGA)_2]^{3-}$ complex started to form with a maximum concentration *ca.* 75% at pH 9.8. The formation of these two-species together with the protonated complex $[Eu(HGA)H]^{+}$ that formed at pH range (4.0–10.0), was able to suppress the formation of the hydroxide species, $Eu(OH)^{+2}$, $Eu(OH)_2^{+}$, and $Eu(OH)_3$, in the pH range (4.0–10.0). The $Eu(OH)^{+2}$ species found at *ca.* pH 6.0 with very small concentrations not exceeding 0.5%, while the $[Eu(HGA)_3]^{6-}$ complex is formed in the pH range (9.0–12.5). The $Eu(OH)_3$ and $Eu(OH)_4^{-}$ species are formed above pH 10.0. One can conclude from the high stability of Eu(III)–gallic acid complex in aqueous solution that it could be applied in chemotherapy or for the extraction of Eu(III) ion.

Confirmation of the Eu(III)–gallic acid complexes in aqueous solution has been carried out by luminescence measurements. Fig. 6 shows the luminescence spectra of $EuCl_3 \cdot 6H_2O$, [Eu(HGA)], $[Eu(HGA)_2]^{3-}$, and $[Eu(HGA)_3]^{6-}$ at the pH values of their maximum formations. The europium salt showed two emission bands between 400 nm and 800 nm. The first band is strong and appears at ~731 nm, while the second band is weak and appears at 417 nm. The intensity

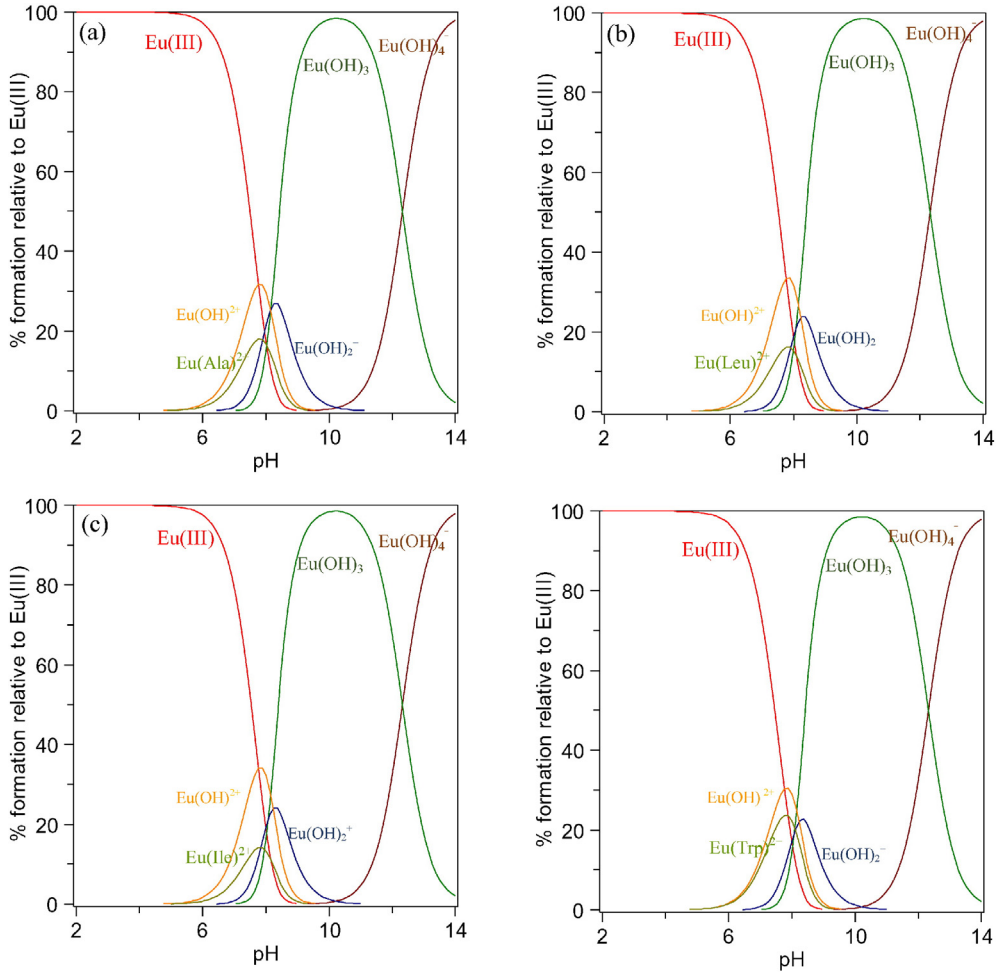

Fig. 8. Species-distribution diagrams of Eu(III) with (a) Ala, (b) Leu, (c) Ile, and (d) Trp; [Eu(III)] = $4 \cdot 10^{-4}$ M and [amino acid] = $1 \cdot 10^{-3}$ M; $I = 0.1$ M $NaNO_3$ and 298.2 K.

of the 731 nm peak of [Eu(HGA)] complex is higher than that of europium salt, and its intensity is reduced in the case of $[Eu(HGA)_2]^{3-}$, and $[Eu(HGA)_3]^{6-}$ complexes. The peak at 417 nm is vanished for $[Eu(HGA)_2]^{3-}$, and $[Eu(HGA)_3]^{6-}$ complexes. The spectra of [Eu(HGA)], $[Eu(HGA)_2]^{3-}$, and $[Eu(HGA)_3]^{6-}$ are different from that of the europium salt, emphasizing their formation in solution.

UV–visible absorption spectra are useful to prove the formation of metal–ion complexes in solution. As a representative, Fig. 7 shows visible absorption spectra of $[Eu(HGA)_2]^{3-}$ at a given pH value. Europium chloride shows almost no absorption spectra in the spectrum range 250–800 nm, whereas gallic acid at pH 9.8 shows two peaks at 330 and 630 nm. These two peaks were shifted to higher wavelength, indicating the formation of $[Eu(HGA)_2]^{3-}$ complex.

The potentiometric studies of amino acids with Eu(III) showed the formation of the species $[Eu(amino\ acid)]^{2+}$. The stability constants of $[Eu(amino\ acid)]^{2+}$ are relatively low with values between 4.42 and 4.72. The best fit was obtained with fixing both protonation constants of amino acids and the hydrolysis constants of Eu(III) ion. Available stability constants for the formation of $[Eu(Ala)]^{2+}$, $[Eu(Leu)]^{2+}$, and $[Eu(Trp)]^{2+}$ complexes are reported in Table 2 [63], which agree with our results. It was reported that the amino acids show, in general, a weak binding to lanthanide metals, and Ln–amino acid binding is mostly electrostatic in nature [67]. The stability constant values are always low, and variations for different amino acids are small [67]. The order of complexation for $[Eu(amino\ acid)]^{2+}$ species was as follows: $[Eu(Ala)]^{2+} > [Eu(Leu)]^{2+} > [Eu(Ile)]^{2+} > [Eu(Trp)]^{2+}$ (Table 2). They exhibit a decrease in the complex strength as the basicity of amino acids decreases. The stability constant of $[Eu(amino\ acid)_2]^{+}$ complexes could not be obtained due to the poor stability of these complexes; hydrolysis reactions are obvious competing processes [67]. The optimized structures of $[EuAla(H_2O)_6]^{+2}$, $[EuLeu(H_2O)_6]^{+2}$, $[EuIle(H_2O)_6]^{+2}$, and $[EuTrp(H_2O)_6]^{+2}$ complexes with DFT/TZVP levels are given in Fig. S11. The SDD for 1:2.5 (Eu(III): amino acid) molar ratios shown in Fig. 8 was generated with the stability constants of $[Eu(amino\ acid)]^{2+}$ and hydrolyzed Eu(III) complexes summarized in Table 2. These speciation calculations reveal that the $[Eu(amino\ acid)]^{2+}$ complex coexists in low concentration (<23% at *ca.* pH 7.4) and the predominant species are the mononuclear hydroxides.

The complex formation between the Eu(III), gallic acid, and amino acid (Ala, Leu, Ile, or Trp) at a 1:1:1 molar ratio has also been studied potentiometrically and the best model to fit the potentiometric data suggests the presence of the following species: [Eu(HGA)(amino acid)H], $[Eu(HGA)(amino\ acid)]^{-}$, and $[Eu(HGA)(amino\ acid)H_{-1}]^{2-}$. These species were obtained by fixing the previously estimated hydrolysis constants of Eu(III) and the protonation constants of gallic acid and amino acid, as well as the stability constants of their complexes with Eu(III). The simultaneously refined values of $\log\beta_{1111}$, $\log\beta_{1110}$, and $\log\beta_{111-1}$ are given in Table 2, and the corresponding SDDs for the 1:1:1 molar ratios are shown in Fig. 9. These SDDs clearly show that these mixed complexes are indeed formed with significant concentrations, and thus hinder the formation of the hydrolysis constants of Eu(III) ion in the pH range of *ca.* pH (4–10). The [Eu(HGA)(amino acid)H] is the predominant complex of all species and reached maximum (*ca.* 75%) at the physiological pH 7.4. At the same pH the

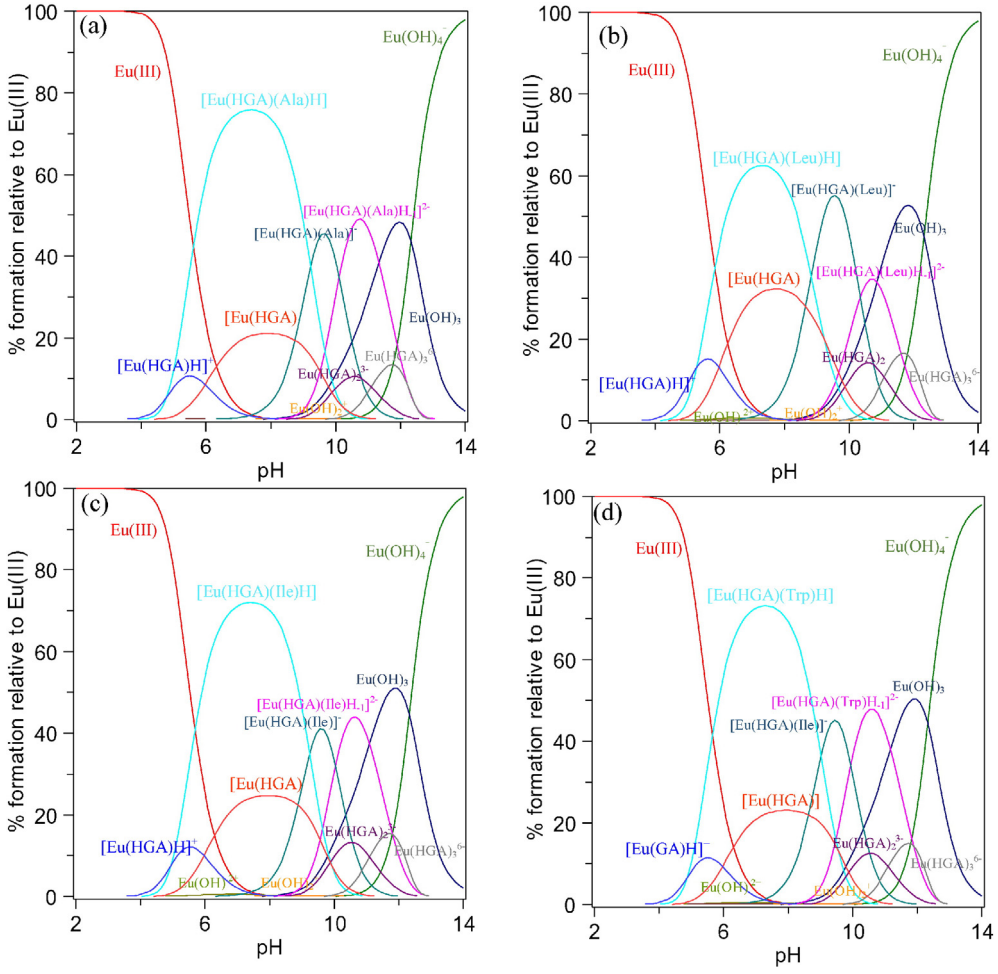

Fig. 9. Species-distribution diagrams of Eu(III) with (a) gallic acid–Ala system, (b) gallic acid–Leu system, (c) gallic acid–Ile system, and (d) gallic acid–Trp system; [Eu(III)] = [gallic acid] = [amino acid] = $1 \cdot 10^{-3}$ M; $I = 0.1$ M $NaNO_3$ and 298.2 K.

[Eu(HGA)] complex coexists in notable concentration (*ca.* 21%). The ternary complexes $[Eu(HGA)(amino\ acid)]^{-}$ and $[Eu(HGA)(amino\ acid)H_{-1}]^{2-}$ were formed at pH 9.7 and 10.7, respectively. The optimized structures of $[Eu(HGA)(Ala)(H_2O)_4]^{-}$, $[Eu(HGA)(Leu)(H_2O)_4]^{-}$, $[Eu(HGA)(Ile)(H_2O)_4]^{-}$, and $[Eu(HGA)(Trp)(H_2O)_4]^{-}$ complexes with DFT/TZVP levels are plotted in Fig. S12.

4. Conclusion

In this work, the complexation between Eu(III), gallic acid, alanine, leucine, isoleucine, and tryptophan was studied potentiometrically at 298.2 K and ionic strength $I = 0.1$ M $NaNO_3$. The protonation constants of gallic acid and amino acids were calculated from the potentiometric data, and compared with the predictions using the COSMO-RS model. The predicted values were shown to be in good agreement with the experimental values. The stability constants of the mononuclear hydroxyl complexes, $Eu(OH)^{2+}$, $Eu(OH)_2^{+}$, $Eu(OH)_3$, and $Eu(OH)_4^{-}$ were obtained. The potentiometric data revealed that gallic acid acts as a strong chelator for Eu(III). The Eu(III)–gallic acid complex could be a promising chemotherapeutic drug due to its high stability. The $[Eu(HGA)H]^{+}$, $[Eu(HGA)]$, $[Eu(HGA)_2]^{3-}$, and $[Eu(HGA)_3]^{6-}$ complexes were obtained, and their overall stability constants were found to be 17.29, 11.33, 17.23, and 21.52, respectively. The stability constants of the binary Eu(III) + amino acid systems and the ternary Eu(III) + gallic acid + amino acid systems were calculated. The $[Eu(amino\ acid)]^{2+}$ complex was formed in the former systems, while the species $[Eu(HGA)(amino\ acid)H]$, $[Eu(HGA)(amino\ acid)]^{-}$, and $[Eu(HGA)(amino\ acid)H_{-1}]^{2-}$ were formed in the latter ones. The species distribution diagrams of the obtained complexes in solution were computed.

Acknowledgment

This work was financed by national funding from Fundação para a Ciência e a Tecnologia (FCT, Portugal), European Union, QREN, FEDER and COMPETE for funding the CICECO (project PEst-C/CTM/LA0011/2013), QOPNA (project PEst-C/QUI/UI0062/2013) and LSRE/LCM (project PEst-C/EQB/LA0020/2013). M. Taha and I. Khan acknowledge FCT for the postdoctoral grants SFRH/BPD/78441/2011 and SFRH/BPD/76850/2011, respectively.

Appendix A. Supplementary data

Supplementary data to this article can be found online at http://dx.doi.org/10.1016/j.jinorgbio.2016.01.017.

References

[1] G. Zhang, J. Guo, J. Pan, X. Chen, J. Wang, J. Mol. Struct. 923 (2009) 114–119.
[2] X.-Q. He, Q.-Y. Lin, R.-D. Hu, X.-H. Lu, Spectrochim. Acta, Part A 68 (2007) 184–190.
[3] G.-J. Chen, X. Qiao, C.-Y. Gao, G.-J. Xu, Z.-L. Wang, J.-L. Tian, J.-Y. Xu, W. Gu, X. Liu, S.-P. Yan, J. Inorg. Biochem. 109 (2012) 90–96.
[4] T.W. Hambley, Coord. Chem. Rev. 166 (1997) 181–223.
[5] E. Wong, C.M. Giandomenico, Chem. Rev. 99 (1999) 2451–2466.
[6] D.-D. Qin, G.-F. Qi, Z.-Y. Yang, J.-C. Wu, Y.-c. Liu, J. Fluoresc. 19 (2009) 409–418.
[7] I. Hemmilä, V. Laitala, J. Fluoresc. 15 (2005) 529–542.
[8] O. Kutsenko, V. Trusova, G. Gorbenko, T. Deligeorgiev, A. Vasilev, S. Kaloianova, N. Lesev, J. Fluoresc. 21 (2011) 1689–1695.
[9] C.M. Cummins, M.E. Koivunen, A. Stephanian, S.J. Gee, B.D. Hammock, I.M. Kennedy, Biosens. Bioelectron. 21 (2006) 1077–1085.
[10] K. Matsumoto, T. Nojima, H. Sano, K. Majima, Macromol. Symp. 186 (2002) 117–121.
[11] A.B. Caballero, A. Rodríguez-Diéguez, J.M. Salas, M. Sánchez-Moreno, C. Marín, I. Ramírez-Macías, N. Santamaría-Díaz, R. Gutiérrez-Sánchez, J. Inorg. Biochem. 138 (2014) 39–46.
[12] F. Albaaj, A.J. Hutchison, Expert. Opin. Pharmacother. 6 (2005) 319–328.
[13] C.H. Evans, Trends Biochem. Sci. 8 (1983) 445–449.
[14] K. Wang, Y. Cheng, X. Yang, R. Li, Met. Ions Biol. Syst. 40 (2003) 707–751.
[15] Y. Mawani, C. Orvig, J. Inorg. Biochem. 132 (2014) 52–58.
[16] V. Trusova, A. Yudintsev, L. Limanskaya, G. Gorbenko, T. Deligeorgiev, J. Fluoresc. 23 (2013) 193–202.
[17] I. Kostova, Curr. Med. Chem.: Anti-Cancer Agents 5 (2005) 591–602.
[18] G. Momekov, T. Deligeorgiev, A. Vasilev, K. Peneva, S. Konstantinov, M. Karaivanova, Med. Chem. 2 (2006) 439–445.
[19] I.A. Boldyrev, G.P. Gaenko, E.V. Moiseeva, T. Deligeorgiev, S. Kaloyanova, N. Lesev, A. Vasilev, J.G. Molotkovsky, Russ. J. Bioorg. Chem. 37 (2011) 364–368.
[20] H.A. Azab, S.S. Al-Deyab, Z.M. Anwar, R.G. Ahmed, J. Chem. Eng. Data 56 (2010) 833–849.
[21] K.-C. Choi, Y.-H. Lee, M.G. Jung, S.H. Kwon, M.-J. Kim, W.J. Jun, J. Lee, J.M. Lee, H.-G. Yoon, Mol. Cancer Res. 7 (2009) 2011–2021.
[22] N. Jiménez, J.A. Curiel, I. Reverón, B. de las Rivas, R. Muñoz, Appl. Environ. Microbiol. 79 (2013) 4253–4263.
[23] M.-S. Kang, J.-S. Oh, I.-C. Kang, S.-J. Hong, C.-H. Choi, J. Microbiol. 46 (2008) 744–750.
[24] J.M. Kratz, C.R. Andrighetti-Fröhner, P.C. Leal, R.J. Nunes, R.A. Yunes, E. Trybala, T. Bergström, C.R.M. Barardi, C.M.O. Simões, Biol. Pharm. Bull. 31 (2008) 903–907.
[25] S. Habtemariam, A. Sureda, A. Hajizadeh Moghaddam, S. Fazel Nabavi, S. Mohammad Nabavi, F. Abolhasani, Lett. Drug Des. Discovery 10 (2013) 277–282.
[26] S. Nabavi, S. Habtemariam, S. Nabavi, A. Sureda, M. Daglia, A. Moghaddam, M. Amani, Mol. Cell. Biochem. 372 (2013) 233–239.
[27] J.-D. Hsu, S.-H. Kao, T.-T. Ou, Y.-J. Chen, Y.-J. Li, C.-J. Wang, J. Agric. Food Chem. 59 (2011) 1996–2003.
[28] B. You, S. Kim, S. Kim, W. Park, Mol. Cell. Biochem. 357 (2011) 295–303.
[29] D.K. Maurya, N. Nandakumar, T.P.A. Devasagayam, J. Clin. Biochem. Nutr. 48 (2011) 85–90.
[30] K. Liu, A.-C. Huang, P.-P. Wu, H.-Y. Lin, F.-S. Chueh, J.-S. Yang, C.-C. Lu, J.-H. Chiang, M. Meng, J.-G. Chung, Oncol. Rep. 26 (2011) 177–184.
[31] T.-T. Ou, C.-J. Wang, Y.-S. Lee, C.-H. Wu, H.-J. Lee, Mol. Nutr. Food Res. 54 (2010) 1781–1790.
[32] B.R. You, H.J. Moon, Y.H. Han, W.H. Park, Food Chem. Toxicol. 48 (2010) 1334–1340.
[33] B.R. You, W.H. Park, J. Agric. Food Chem. 59 (2010) 763–771.
[34] A. Faried, D. Kurnia, L.S. Faried, N. Usman, T. Miyazaki, H. Kato, H. Kuwano, Int. J. Oncol. 30 (2007) 605–613.
[35] M. López-Lázaro, J.M. Calderón-Montaño, E. Burgos-Morón, C.A. Austin, Mutagenesis (2011) 1–10.
[36] C.-L. Liao, K.-C. Lai, A.-C. Huang, J.-S. Yang, J.-J. Lin, S.-H. Wu, W. Gibson Wood, J.-G. Lin, J.-G. Chung, Food Chem. Toxicol. 50 (2012) 734–1740.
[37] C.-Z. Liang, X. Zhang, H. Li, Y.-Q. Tao, L.-J. Tao, Z.-R. Yang, X.-P. Zhou, Z.-L. Shi, H.-M. Tao, Cancer Biother. Radiopharm. 27 (2012) 701–710.
[38] L. Lo, M. Yang, C. Weng, C. Lin, Int. J. Oncol. 37 (2010) 377–385.
[39] C. Locatelli, P.C. Leal, R.A. Yunes, R.J. Nunes, T.B. Creczynski-Pasa, Chem. Biol. Interact. 181 (2009) 175–184.
[40] D. Lamoral-Theys, L. Pottier, F. Kerff, F. Dufrasne, F. Proutière, N. Wauthoz, P. Neven, L. Ingrassia, P.V. Antwerpen, F. Lefranc, M. Gelbcke, B. Pirotte, J.-L. Kraus, J. Nève, A. Kornienko, R. Kiss, J. Dubois, Bioorg. Med. Chem. 18 (2010) 3823–3833.
[41] A. Sharma, S.P. Gautam, A.K. Gupta, Bioorg. Med. Chem. 19 (2011) 3341–3346.
[42] A.E. Fazary, Hernowo, A. Angkawijaya, T.-C. Chou, C. Lin, M. Taha, Y.-H. Ju, J. Solut. Chem. 40 (2011) 1965–1986.
[43] A.E. Angkawijaya, A.E. Fazary, S. Ismadji, Y.-H. Ju, J. Chem. Eng. Data 57 (2012) 3443–3451.
[44] A.E. Fazary, M. Taha, Y.-H. Ju, J. Chem. Eng. Data 54 (2009) 35–42.
[45] F.S. Rehmani, Z.T. Maqsood, S.A. Kazmi, J. Chem. Soc. Pak. 19 (1997) 38–41.
[46] N.N. Sergeeva, M. Donnier-Marechal, G. Vaz, A.M. Davies, M.O. Senge, J. Inorg. Biochem. 105 (2011) 1589–1595.
[47] A. Braibanti, G. Ostacoli, P. Paoletti, L.D. Pettit, S. Sammartano, Pure appl. Chem. (1987) 1721–1728.
[48] O. Yamauchi, A. Odani, Pure appl. Chem. (1996) 469–496.
[49] S. Sjöberg, Pure appl. Chem. (1997) 1549–1570.
[50] P. Gans, B. O'Sullivan, Talanta 51 (2000) 33–37.
[51] R.F. Jameson, M.F. Wilson, J. Chem. Soc. Dalton Trans. (1972) 2610–2614.
[52] P. Gans, A. Sabatini, A. Vacca, Talanta 43 (1996) 1739–1753.
[53] L. Alderighi, P. Gans, A. Ienco, D. Peters, A. Sabatini, A. Vacca, Coord. Chem. Rev. 184 (1999) 311–318.
[54] A. Schafer, A. Klamt, D. Sattel, J.C.W. Lohrenz, F. Eckert, Phys. Chem. Chem. Phys. 2 (2000) 2187–2193.
[55] A. Klamt, J. Phys. Chem. 99 (1995) 2224–2235.
[56] A. Klamt, V. Jonas, T. Bürger, J.C.W. Lohrenz, J. Phys. Chem. A 102 (1998) 5074–5085.
[57] A. Klamt, F. Eckert, M. Diedenhofen, M.E. Beck, J. Phys. Chem. A 107 (2003) 9380–9386.
[58] M. Dolg, H. Stoll, A. Savin, H. Preuss, Theor. Chim. Acta 75 (1989) 173–194.
[59] A. Eslami, W. Pasanphan, B. Wagner, G. Buettner, Chem. Cent. J. 4 (2010) 15.
[60] H. Powell, M. Taylor, Aust. J. Chem. 35 (1982) 739–756.
[61] D. Perrin, Stability constants of metal–ion complexes, Part B: Organic ligands, Pergamon Press, Oxford, 1979 in,.
[62] T. Marino, A. Galano, N. Russo, J. Phys. Chem. B 118 (2014) 10380–10389.
[63] L.D. Pettit, K. Powell, IUPAC stability constants database, Chem. Int. (2006).
[64] A. Klamt, F. Eckert, M. Diedenhofen, M.E. Beck, J. Phys. Chem. A 107 (2003) 9380–9386.
[65] F. Eckert, A. Klamt, J. Comput. Chem. 27 (2006) 11–19.
[66] M.H. Bradbury, B. Baeyens, Geochim. Cosmochim. Acta 66 (2002) 2325–2334.
[67] H.A. Azab, S.S. Al-Deyab, Z.M. Anwar, I.I. Abd El-Gawad, R.M. Kamel, J. Chem. Eng. Data 56 (2011) 2613–2625.